Materials Letters 285 (2021) 129191

Contents lists available at ScienceDirect

Materials Letters

journal homepage: www.elsevier.com/locate/mlblue

Electrochemical signature of CuS photosensitizers thermalized from alkyldithiocarbamato Cu(II) molecular precursors for quantum dots sensitized solar cells

Mojeed A. Agoro [a,b,*], Johannes Z. Mbese [a], Edson L. Meyer [b], Kevin Onyenankeya [c]

[a] Department of Chemistry, University of Fort Hare, Private Bag X1314, Alice 5700, South Africa
[b] Fort Hare Institute of Technology, University of Fort Hare, Private Bag X1314, Alice 5700, South Africa
[c] Department of Communication, University of Fort Hare, Alice, South Africa

ARTICLE INFO

Article history:
Received 20 October 2020
Received in revised form 2 December 2020
Accepted 5 December 2020
Available online 10 December 2020

Keywords:
Photovoltaic
Semiconductor
Nanomaterials
Optical
Electrochemistry

ABSTRACT

Environmental friendly and affordable energy sources is one of the biggest challenges of modern society. The substantial negative impact of fossil fuels on the environment has prompted the need for clean and sustainable solar energy. Recent reports affirm that increase in photovoltaic conversion efficiency is directly linked to morphology control resulting in excellent catalytic activity on the active layer. Herein, we report on the fabrication of (H is the addition of hexadecylamine HDA capping agents CuS-H) and (CuS without HDA) photosensitizers using molecular precursor approach. The obtained CuS-H and CuS were characterized using structural, morphological and electrochemical instruments. The CV, EIS and bode plot results show that CuS displayed stronger electrocatalytic activity as a good optimum sensitizer. *J-V* efficiency obtained indicates that the CuS exhibited a much better efficiency in the QDSCs compared to CuS-H.

1. Introduction

In the last decade, energy production, distribution and security have come to occupy an important place in most societies [1]. This has heightened the search for efficient energy conversion materials that are not only environmentally friendly and cost-effective, but also capable of resolving the energy crisis [2]. This account for the increasing interest in materials with photovoltaic conversion efficiency such as Copper sulfide (CuS) nanoparticles. In various fields such as solar cells, photocatalytic degradation, superconductors and optical filters [3], there is a tremendous attraction for CuS nanoparticles because of their small size, excellent electronic and optical properties. Their small size has displayed novel electronic physical, chemical, magnetic, and surface properties compared to the bulk nanoparticles properties. Besides, photovoltaic relies on the morphology of the active layer to increase power conversion efficiency [4]. Various approaches have been used to fabricate CuS nanoparticles such as polyol, microwave irradiation, convenient solution process, molecular precursor, chemical vapour deposition, hydrothermal, etc... [5,6]. One of the most promising approaches is molecular precursor, which is cost-friendly and efficient with interesting morphology [7]. It uses the aid of capping agents to control the morphology of the nanoparticles and obtain small particle sizes, which is vital for different applications [8]. In the present study, the electrochemical signature of CuS photosensitizers was explored to ascertain their beneficial effects in quantum dots sensitized solar cells.

2. Experimental

Two approaches were adopted to synthesize CuS-H and CuS photosensitizers. CuS-H was achieved by a slight modification of literature by [8]. 3 g of hot HDA was mixed with 0.20 g of (alkyldithiocarbamato) Cu(II) and 4 mL oleic acid (OA) at 360 °C for 1 h. The reaction mixture was dropped to 70 °C and washed with 25 mL methanol through centrifugation to remove excess HDA and OA, followed by air drying and the final product of CuS-H obtained. Perkin Elmer TGA 4000 ThermoGravimetric Analyser was employed to fabricate CuS. 25 mg of (alkyldithiocarbamato) Cu(II) was loaded into an alumina pan at a temperature gradient between 30 and 900 °C. At temperatures between 360 and 900 °C with a gas flowing of nitrogen at a rate of 20 mL min^{-1}, CuS was formed from the final residue. Assembling of QDSC was achieved with 2 × 2 cm^2 FTO of Platinum and TiO_2 electrodes with

* Corresponding author at: Department of Chemistry, University of Fort Hare, Private Bag X1314, Alice 5700, South Africa.
E-mail address: magoro@ufh.ac.za (M.A. Agoro).

https://doi.org/10.1016/j.matlet.2020.129191
0167-577X/

6 × 6 mm^2 active areas of TiO_2 screen coated. Dye loading was done using CuS-H and CuS in 10 mL of warm water with chenodeoxycholic acid and addictive co-adsorbents. The TiO_2 FTO was soaked into the solution of CuS-H and CuS for 24 h. The platinum electrode and the TiO_2 loaded with CuS-H and CuS were held together using polyethylene and soldering iron. The syringe was used to inject the HI-30 electrolyte iodide at 0.05 M. Electrochemical studies were carried out using Metrohm 85695 Autolab with Nova 1.10 software. Platinum (as counter electrode), TiO_2 (as anode electrode) and HI-30 iodide (as reference electrode) were used. Cyclic voltammetry (CV) was carried out at scan rates between 0.05 and 0.35 V s^{-1} with an increment of 0.05 V s^{-1}. Electrochemical Impedance Spectroscopy (EIS) was performed at 100 kHz to 100. Keithley 2401 source meter and a Thorax light power meter evaluated current density-voltage (*J-V*) parameters. Lumixo AM1.5 light simulator was employed and lamp was fixed at 50 cm high to avoid illumination outside of the working area. X-ray diffraction (XRD) was used to explore the structural pattern, between 10 and 90° at 40 kV and 40 mA using Cu-Kα radiation (λ = 0.15406 nm). JEOL JEM 2100 Transmission Electron Microscope (TEM) operating at 200 kV. Scanning Electron Microscope (SEM) Zeiss Auriga SEM outfitted with Energy Dispersive X-Ray Spectroscopy (EDX) with Smart SEM programming was utilized at a quickening voltage of 30 kV. Perkin Elmer LAMBDA 365 UV–Vis spectrophotometer were used to measure optical properties. The photoluminescence of the samples was done through Perkin Elmer LS 45 fluorimeter.

3. Results and discussion

XRD was adopted to investigate the structure and phase pattern of CuS-H and CuS materials, see Fig. 1(a, e). The characteristic diffraction peaks of CuS-H exhibited at 11.70°–81.80° and 26.6°–84° for CuS both corresponding to the indexed of hexagonal covellite phases of CuS (JCPDS no. 00-006-0464). Dunne et al., established that temperature sizes dependent nanoparticles are obtained by either nucleation or growth dominated route [9]. SEM images of CuS-H and CuS are shown in Fig. 1(b, f). Both CuS and CuS-H displayed densely clusters packed particles with a better crystalline, well micron-size and regular-shaped particles. This is linked to the effect of high temperature and molecular precursor due to their long-chain carbon, affirmed by the report of [10]. The EDX spectral of both CuS and CuS-H nanoparticles confirmed the presence of C and O as seen in Fig. 1(c, g). It is observed that the elemental composition weight of Cu and S are a little higher in CuS photosensitizer than CuS-H. TEM images of CuS-H and CuS nanoparticles as seen in Fig. 1(d, h). CuS-H reveals agglomerated nanoparticles (Fig. 1d), linked to excess capping agent with an average size of 18.98–57.63 nm. CuS image depicts a spherical shape with crystallite sizes between 6.89 and 13.56 nm as seen in (Fig. 1h), which agrees with the study by [11].

Fig. 2(a, d), presents CV curves of CuS-H and CuS photosensitizers. The CV curves of both samples exhibit two pairs of redox peaks, the cathodic and anodic peak. CuS-H was slightly less than that of the CuS. However, CuS sensitizer exhibited higher current density than CuS-H sensitizer in their redox peaks. This is capable of enhancing CuS complexion with TiO_2 surface, which promotes conversion efficiency [12]. The EIS as seen in Fig. 2(b, e), revealed a high-frequency region with no small semicircle, which means that CuS displaces insignificant charge transfer resistance. CuS-H with straight line connotes electronic conductivity and higher ionic. This implies that CuS-H catalytic activity is poor [13]. The electron diffusion rate and the longer lifetime of CuS depicted that the τ values are larger Thereby, enabling a higher conversion efficiency in QDSCs. The CuS-H (Fig. 2c), lower electron lifetime is linked to recombination through the injected HDA capping agent. The electrons lifetime (τ) for CuS (Fig. 2f), increased due to the highly crystallized structure which is in good agreement with XRD result [14]. Fig. 3(b, e), shows the emission spectra of CuS-H displays blue and red shift at 451–691 nm and 453–614 nm for CuS. This is due to the microstructure and chemical composition of the material, which is similar to the studies by [15]. UV–Vis spectra (Fig. 3(c, f), displays absorption around 268–271 nm for CuS and CuS-H absorption band edges at 274 nm, which is similar to the study by [16]. *J-V* characteristics of CuS-H and CuS are shown in Table 1 and Fig. 3(a, d). *J-V* efficiency obtained indicates that the photosensitizer of CuS has a much output performance compared to CuS-H. The active surface area increases the catalyst

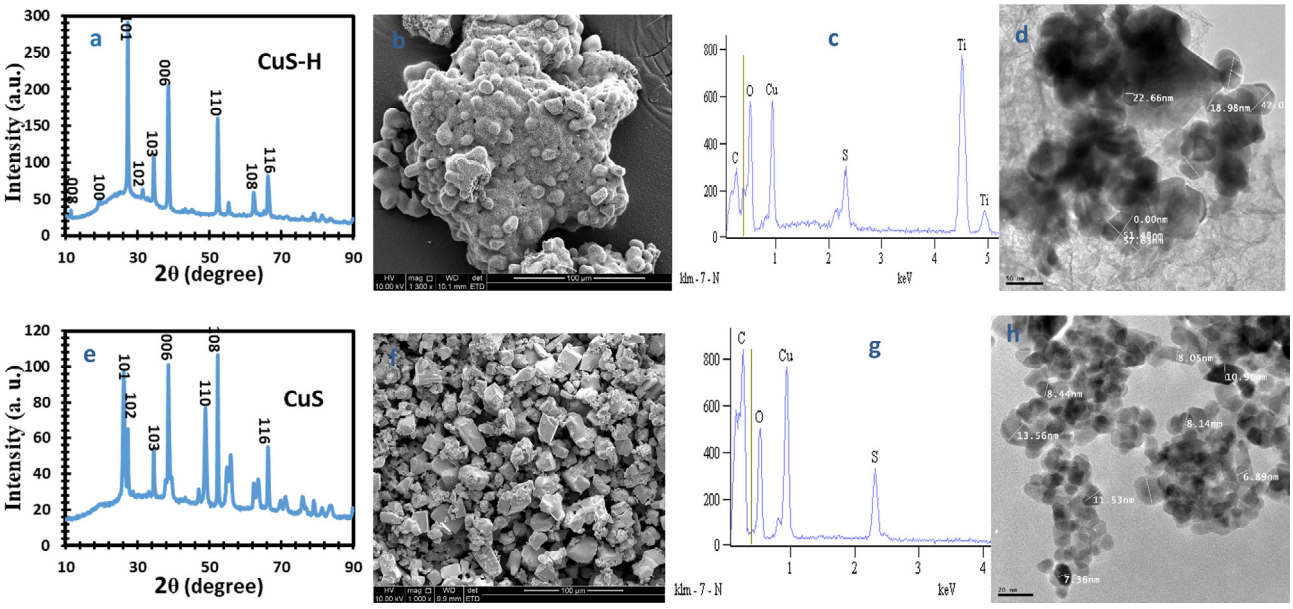

Fig. 1. (a, e) XRD, (b, f) SEM, (c, g) EDX, (d, h) HR-TEM of CuS-H and CuS respectively.

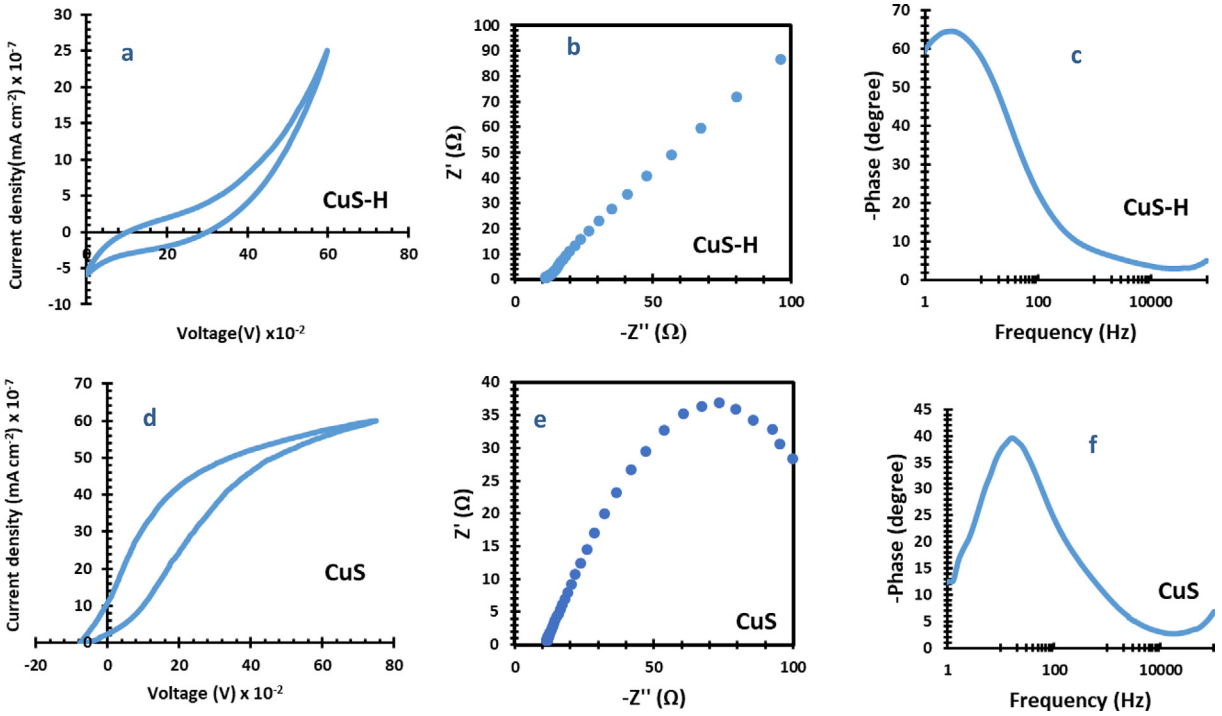

Fig. 2. (a, d) CV, (b, e) EIS, (c, f) Bode plot of CuS-H and CuS respectively.

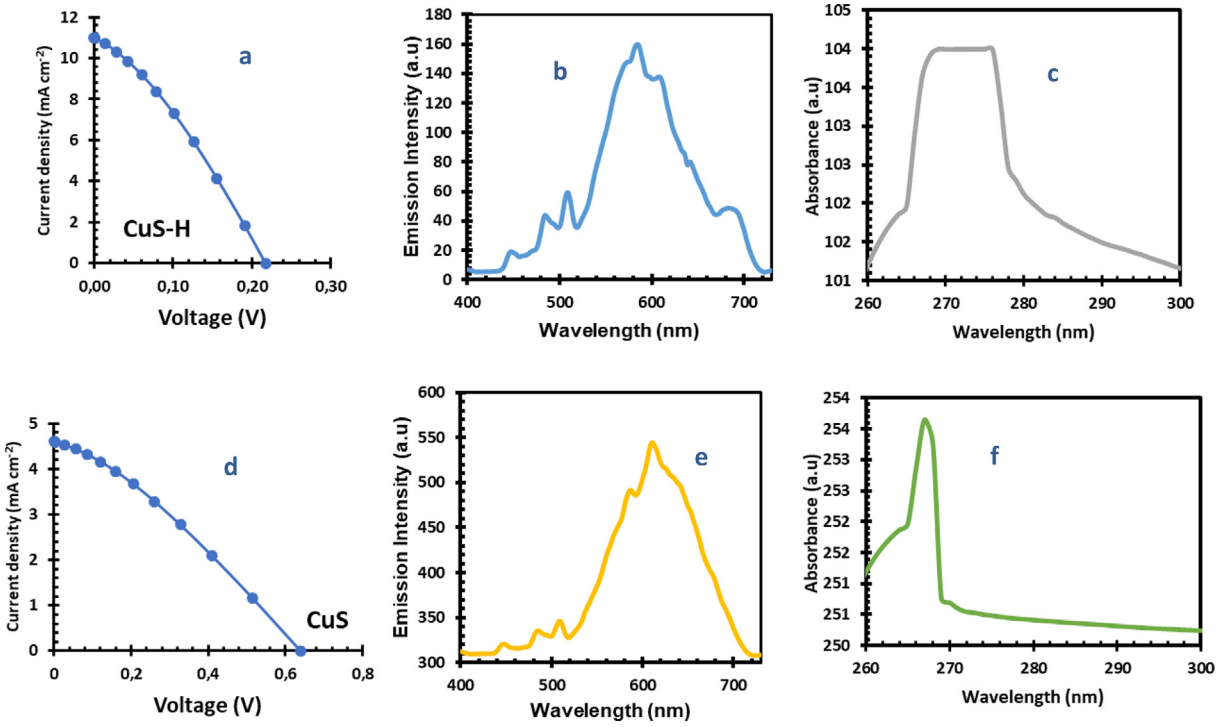

Fig. 3. (a, d) *I-J*, (b, e) PL, (c, f) U-Vis of CuS-H and CuS respectively.

of materials with an increase in Jsc as seen in CuS-H 11 cm^{-1}. CuS exhibited a much better efficiency in the QDSCs with higher *Voc* and highest η of 0.87%. The higher electron density at TiO_2 conduction band accounts for the higher *Voc* value, which elevates the Fermi level [17].

4. Conclusions

In this study, photosensitizer's nanoparticles were successfully prepared through a molecular precursor route. The cathodic and anodic peaks of CuS-H was slightly less compared to CuS. The EIS

Table 1
J–V characteristics of CuS-H and CuS nanoparticles.

Dye	Photoanode	Electrolyte	CEs	J_{SC} (mA/cm^2)	V_{OC} (V)	*FF*	η (%)
CuS-H	TiO_2	HI-30	Pt	11	0.218	0.311	0.75
CuS	TiO_2	HI-30	Pt	4.559	0.678	0.279	0.87
Previous study [8]							
CUS/HDA	TiO_2	HI-30	Pt	1.78	0.877	0.1	0.15
CUS	TiO_2	HI-30	Pt	0.64	0.068	0.3	0.01

results show that CuS-H displayed insignificant charge transfer resistance. While CuS sensitizer exhibited reversed change tendency and semicircle exchange current density of *Rs*, and *Rct* as well as optimum sensitizer. *J-V* efficiency obtained indicates that the CuS exhibited a much better efficiency in the QDSCs with higher *Voc* and highest η of 0.87%. CuS displayed stronger electrocatalytic activity as a well optimum sensitizer. Although, the electrochemical performance of both photosensitizers is not the most impressive one. However, the obtained efficiency is enhanced compared to the previous study [8].

Funding

This research was funded by the National Department of Science and Innovation, South Africa (DST/CON 0170/2019), National Research Foundation, South Africa (GUN: 93215), Govan Mbeki Research and Development Centre (GMRDC) at the University of Fort Hare, South Africa, Eskom TESP, South Africa (P948) and NRF Thuthuka Grant, South Africa (GUN: 118139).

Declaration of Competing Interest

The authors declare that they have no known competing financial interests or personal relationships that could have appeared to influence the work reported in this paper.

References

[1] A.S. Jadhav, V.M. Bhuse, Bull. Mater. Sci. 42 (2019) 12.
[2] Y.J. Wang, D.P. Wilkinson, J. Zhang, Chem. Rev. 111 (2011) 7625–7651.
[3] C. Nethravathi, R.R. Nath, J.T. Rajamathi, M. Rajamathi, ACS Omega 4 (2019) 4825–4831.
[4] Y. Fan, Y. Li, X. Han, X. Wu, L. Zhang, Q. Wang, Molecules 24 (2019) 3776.
[5] F. Zhao, C. Wang, X. Zhan, Adv. Energy Mater. 8 (2018) 1703147.
[6] E.L. Meyer, J.Z. Mbese, M.A. Agoro, Molecules 24 (2019) 4223.
[7] T. Marimuthu, N. Anandhan, R. Panneerselvam, K.P. Ganesan, A.A. Roselin, Nano-Struct. Nano-Objects 17 (2019) 138–147.
[8] M.A. Agoro, E.L. Meyer, J.Z. Mbese, K. Manu, Catalysts 10 (2020) 300.
[9] P.W. Dunne, C.L. Starkey, M. Gimeno-Fabra, E.H. Lester, Nanoscale 6 (2014) 2406–2418.
[10] M. Akhtar, Y. Alghamdi, J. Akhtar, Z. Aslam, N. Revaprasadu, M.A. Malik, Mater. Chem. Phys. 180 (2016) 404–412.
[11] F.F. Castillón-Barraza, M.H. Farías, J.H. Coronado-López, M.A. Encinas-Romero, M. Pérez-Tello, R. Herrera-Urbina, A. Posada-Amarillas, Adv. Sci. Lett. 4 (2011) 596–601.
[12] M. Mohammadnezhad, G.S. Selopal, N. Alsayyari, R. Akilimali, F. Navarro-Pardo, Z.M. Wang, B. Stansfield, H. Zhao, F. Rosei, J. Electrochem. Soc. 166 (2019) H3065–H3073.
[13] P. Naveenkumar, G.P. Kalaignan, S. Arulmani, S. Anandan, J. Mater. Sci.: Mater. Electron. 29 (2018) 16853–16863.
[14] H.J. Kim, L. Myung-Sik, C.V. Gopi, M. Venkata-Haritha, S.S. Rao, S.K. Kim, Dalton Trans. 44 (2015) 11340–11351.
[15] M. Saranya, C. Santhosh, R. Ramachandran, P. Kollu, P. Saravanan, M. Vinoba, S. K. Jeong, A.N. Grace, Powder Technol. 252 (2014) 25–32.
[16] P. Chakraborty, J. Adhikary, S. Chatterjee, B. Biswas, T. Chattopadhyay, Rasayan J. Chem. 9 (2016) 77–83.
[17] H. Heydari, S.E. Moosavifard, M. Shahraki, S. Elyasi, J. Energy Chem. 26 (2017) 762–767.